Send Orders for Reprints to reprints@benthamscience.net

Recent Advances in Computer Science and Communications, **XXXX,** *XX,* **1-12**

RESEARCH ARTICLE

Pneumonia Net: Pneumonia Detection and Categorization in Chest X-ray Images

Somya Srivastava[1,*], Seema Verma[2], Nripendra Narayan Das[3], Shraddha Sharma[4] and Gaurav Dubey[5]

[1]Department of Computer Science, ABES Engineering College, Ghaziabad, India; [2]Department of Computer Science and Engineering, Guru Gobind Singh Indraprastha University, Delhi, India; [3]Department of Information Technology, Manipal University Jaipur, Jaipur, Rajasthan, India; [4]Department of Computer Science, Pandit Deendayal Energy University, Gujarat, India; [5]Department of Computer Science, KIET Group of Institutions, Ghaziabad, India

ARTICLE HISTORY

Received: June 30, 2023
Revised: August 23, 2023
Accepted: September 26, 2023

DOI:
10.2174/0126662558269484231121112300

Abstract: ***Background*:** Pneumonia is one of the leading causes of death and disability due to respiratory infections. The key to successful treatment of pneumonia is in its early diagnosis and correct classification. PneumoniaNet is a unique deep-learning model based on CNN for identifying pneumonia on chest X-rays.

***Objective*:** A deep learning model that combines convolutional, pooling, and fully connected layers is presented in this study.

***Methods*:** In order to learn how to identify cases of pneumonia and healthy controls on chest X-ray pictures, PneumoniaNet was trained on a large labeled library of such images. A robust data augmentation technique was adopted to enhance the model generalization and training set diversity. Standard measures like as accuracy, precision, recall, and F1-score were applied to PneumoniaNet's performance evaluation.

***Results*:** The suggested model performed effectively in detecting pneumonia cases with an accuracy of 93.88%.

***Conclusion*:** The model was evaluated against the current state-of-art methods and showed that PneumoniaNet outperformed the other models.

Keywords: Machine learning, CNNs, prediction model, healthcare, pneumonia, X-ray.

1. INTRODUCTION

Pneumonia is a leading cause of death and disability, especially in young children and the elderly [1]. Pneumonia is an airway infection that can affect anybody, but it is especially dangerous for those with compromised immune systems. Pneumonia can be caused by a wide variety of microorganisms such as bacteria, viruses, and fungi, with Streptococcus pneumonia being the most common bacterial cause and RSV being the most common viral cause. For effective treatment and to avoid consequences like respiratory failure and sepsis, prompt and correct diagnosis of pneumonia is essential. X-rays (CXRs) are routinely employed in the diagnosis and severity evaluation of pneumonia because they can show telltale infiltrates consolidations in the lung parenchyma [2, 3]. CXR picture interpretation is complex since it necessitates a high level of knowledge, is subject to human error, and varies from interpreter to interpreter [3]. In addition, radiology departments around the world have been stressed by the increased demand for CXR interpretation because of the ongoing COVID-19 epidemic, underscoring the importance of having access to automated, reliable, and efficient methods to aid in clinical decision-making. Medical image analysis, such as the detection and categorization of various disorders in radiographic pictures, has benefited greatly from the application of deep learning, particularly CNN [4]. CNNs are the most famous and well-researched neural networks used for localization, detection, classification and segmentation of medical images. The ability of CNN to automatically learn from spatial features makes it suitable for such purposes. It has been shown in multiple studies that using a convolutional neural network (CNN) to detect pneumonia in CXR pictures can increase diagnosis accuracy while decreasing the burden on radiologists. CheXNet, a 121-layer DenseNet architecture, was created by [5] to detect pneumonia and other thoracic disorders from CXR images at a level of performance comparable to that of a radiologist. Researchers in [6] used a trained CNN model to distinguish between bacterial and viral pneumonia in pediatric CXR pictures, demonstrating that their algorithm was more accurate at making this distinction than human radiology specialists. Recent advancements in deep learning techniques and applications have further established the effectiveness of CNNs in detecting pneumonia and differentiating it from other lung diseases, such as COVID-19. Using a deep learning model trained on X-ray images, [7] proposes an automated technique for detecting COVID-19 patients, with a sensitivity of 98.08% and a specificity of 96.24%. Highly

*Address correspondence to this author at the Department of Computer Science, ABES Engineering College, Ghaziabad, India;
E-mail: somya.srivastava@abes.ac.in

2666-2558/XX $65.00+.00

sensitive and specific detection of COVID-19 instances was achieved using [8]. COVID-Net, a custom deep convolutional neural network trained on CXR images. This study further highlights the potential of CNNs in diagnosing pneumonia and related lung disorders by automatically detecting COVID-19 cases from X-ray pictures using transfer learning with CNNs [9].

PneumoniaNet is a unique Convolutional Neural Network (CNN) model proposed in this study for identifying pneumonia on CXR pictures. Chest X-ray images from patients with bacterial pneumonia, patients with viral pneumonia, and healthy controls were used to train the model. To broaden the training set and enhance the model's generalisation capabilities, a powerful data augmentation technique was put into place. To prove its improved performance in both detection and categorization tasks, we compared PneumoniaNet to existing state-of-the-art approaches. We evaluated its performance using common metrics such as accuracy, precision, recall, and F1-score. PneumoniaNet seeks to improve upon the shortcomings of standard diagnostic methods by providing a faster, more precise, and more trustworthy method of identifying and classifying pneumonia in CXR pictures. The model's capacity to generalize across a wide range of CXR pictures is improved by using a CNN architecture, and the data augmentation technique boosts feature extraction. Our findings add to the expanding literature on deep learning-based diagnostic tools. They may have a major influence on pneumonia management by allowing for the quick, accurate, and automated examination of chest X-ray images. The paper's most significant findings are:

- A powerful CNN model named PneumoniaNet was introduced in the study for identifying pneumonia in chest X-rays. This work addresses a critical issue in global health and helps close a gap in the present research environment.
- A powerful data augmentation approach was used in the study's training phase. This method boosted the model's ability to generalize to new situations, which is especially important for medical imaging tasks with small training datasets.
- The research compared PneumoniaNet to other state-of-the-art models, including CheXNet, DenseNet, InceptionNet, ResNet, VGGNet, and COVID-Net, across a number of criteria. It showed that PneumoniaNet is superior to these models on every metric compared to them.

The rest of the paper is organized as follows: Section 2 gives an insight into recent literature. The detailed methodology and the layer-wise description of a convolutional neural network are reported in section 3. In Section 4, we show how the suggested model performed in comparison to the state-of-the-art approaches used in the evaluation. The overall conclusion of the suggested technique and directions for further work are presented in section 5.

2. LITERATURE REVIEW

Significant progress was made in 2015 using the same dataset we are using here for CNN-based Pneumonia Detection. With the recent advancements in deep learning models and the subsequent availability of enormous datasets, algorithms have been able to complete a variety of medical imaging tasks, including skin cancer classification, hemorrhage identification, arrhythmia detection, and diabetic retinopathy detection. The use of chest X-rays in automated medical diagnosis has recently gained attention. There has been a rise in the application of these techniques to diagnose pulmonary nodules and classify cases of tuberculosis of the lungs. Researchers analyzed the Open AI dataset to see how different convolutional models handled various irregularities. They discovered that a universal deep convolutional network design did not fare well in all cases. The classification accuracy of ensemble models was significantly higher than that of single models, and the deep learning methodology finally outperformed rule-based alternatives.

Attention Modules are a part of [10], making the system more focused. Each attention module's feedforward and feedback attention processes are merged into a single feed-forward process in the bottom-up, top-down feed-forward architecture. The authors used a deep neural network (DNN) and an attention mechanism to identify pneumonia from a chest X-ray (Table **1**) [11-20]. The proposed network generates attention-aware features by combining a DNN architecture with channel and spatial attention modules [21]. The authors analyzed Chest X-ray images with a CNN trained with machine learning and deep learning frameworks to detect signs of lung disease (pneumonia) [22]. Presented ChestX-ray6, a low-throughput convolutional neural network (CNN) for automatic lung opacity, pleural effusion, and pleural pneumonia detection from digital chest X-ray pictures. There are a total of 9,514 images, including both healthy and diseased chest X-rays, in the two databases. To better identify the various lung disorders [23], sorts the chest X-ray image collection into COVID-19, pneumonia, pneumothorax, tuberculosis, and normal categories using eight pre-trained deep learning models based on CNN. There are two steps in the classification process. The Adam optimizer is used to train the CNNs, with a mini-batch size of 32 and a maximum of 30 epochs. The authors applied this trained network to the problem of disease categorization [24]. To better detect pneumothorax in CXR images, the Attention-Based Lightweight Convolutional Neural Network (ALCNN) has been explored. This network is both parameter-efficient and memory-efficient. It makes use of layered convolutional layers and an attention-based approach to fine-tune feature maps for each channel. The authors also looked at the results from three other transfer learning methods and compared them to ALCNN.

A study of the statistical relationship between labels improved prediction accuracy, which in turn improved the performance of a dataset consisting of thirteen photos from a total of fourteen categories. While algorithms have been studied for mining and predicting labels from radiological pictures and reports, the labels applied to those images have traditionally been restricted to illness tags alone [25]. Views from chest X-rays were categorized, and CT and X-ray images were used to segment bodily parts, and research was done on the detection of disease in X-ray images [26]. However, it is conceivable to gain from learning visual qualities from text and developing image descriptions that are on par with how a human would describe them.

Some of the most relevant papers have been summarized below in Table **1**.

3. METHODOLOGY

3.1. Dataset

The dataset is divided into three parts (train, test, validation), which are divided into two further sub-categories for each type of image, *i.e*., Pneumonia and Normal. There are a total of 5,864 X-ray images in jpeg format.

All chest X-ray images were first screened by filtering out all low-quality or unreadable scans before their analysis. Two experts evaluated the diagnoses for the images from the dataset before allowing the images to be used for training the model. Fig. (**1**) describes the sample dataset images of chest X-rays. Another expert also checked the evaluation set for any errors.

The data division is responsible for ensuring that the model is built, fine-tuned, and evaluated in a controlled manner to mitigate the issue of overfitting. Overfitting refers to a situation where a model exhibits high performance on the training data but fails to generalize well to new, unseen data. The inclusion of a validation set serves to mitigate the risk of "data leakage" during the model's creation phase, as it provides an unbiased assessment. Conversely, the test set serves as the definitive gauge of the model's genuine ability to generalize. The data division plays a crucial role, and therefore, in this research work, the data has been divided into 80% for training, 15% for testing and 5 % for validation (Fig. **2**).

Table 1. Summary of Research papers with results.

References	Model	Dataset	Results
Singh *et al*. (2023)[10]	Attention-aware CNN architecture, attention modules, deep neural network (DNN) with attention mechanism	Kaggle chest X-ray dataset	Accuracy: 95.47%, F-score: 0.92
Bhandari *et al*. (2022) [11]	Grad-CAM, LIME, SHAP, 10-fold cross-validation	7132 chest X-ray (CXR) images	Test accuracy: 94.31 ± 1.01%, Validation accuracy: 94.54 ± 1.33%
Hajjej *et al*. (2022) [12]	Machine learning, deep learning techniques, automated diagnostics	Not specified	Accuracy: nearly 96%
Ortiz-Toro *et al*. (2022) [13]	Textural image characterization methods, fractal dimension, radiomics, superpixel-based histon	Not specified	Not explicitly reported
Aktas *et al*. [14]	Deep CNNs	103,468 images with 5 classes (COPD signs, COVID, normal, others, and pneumonia)	COVID accuracy: 97%, Overall accuracy: 81%, Normal: 78%, Abnormal: 88%
Saxena *et al*. [15]	Multiclass deep learning models + XAI	Medical images from IEEE [17] and Kaggle [18] depict people with COVID-19, people with viral pneumonia, and healthy people who have had chest X-rays taken.	Not specified explicitly in the abstract.
Lv *et al*. [16]	Cascade-SEME framework + Regional Learning	Images of chest X-rays for differentiating causes of pneumonia (bacterial, viral, and normal) X-ray data set from the chest (COVID-19) dataset for lung segmentation (1,000 masked chest X-rays)	Improved sensitivity, specificity, accuracy, and F1 scores with SEME structure and regional learning
Hussein, H.I., *et al*. (2023) [17]	Lightweight deep CNN-based models	A large dataset of chest X-ray images	2-class accuracy: 98.55%, 3-class accuracy: 96.83%
Iqbal, A., *et al*. (2023) [18]	TB-UNet - segmentation, TB-DenseNet - classification	3 chest X-ray (CXR) datasets	Segmentation: Precision: 95.74%, Recall: 95.12%, F1score: 89.88%
Kusakunniran, W., *et al*. (2023) [19]	Modified InceptionV3 with self-attention layers	Not specified	Sensitivity: 93%, Specificity: 96%, Accuracy: 96%
Cahyani, D.E., *et al*. (2023) [20]	CNN-BiLSTM combination models	Not specified	Resnet50-BiLSTM: Accuracy: 98.48%

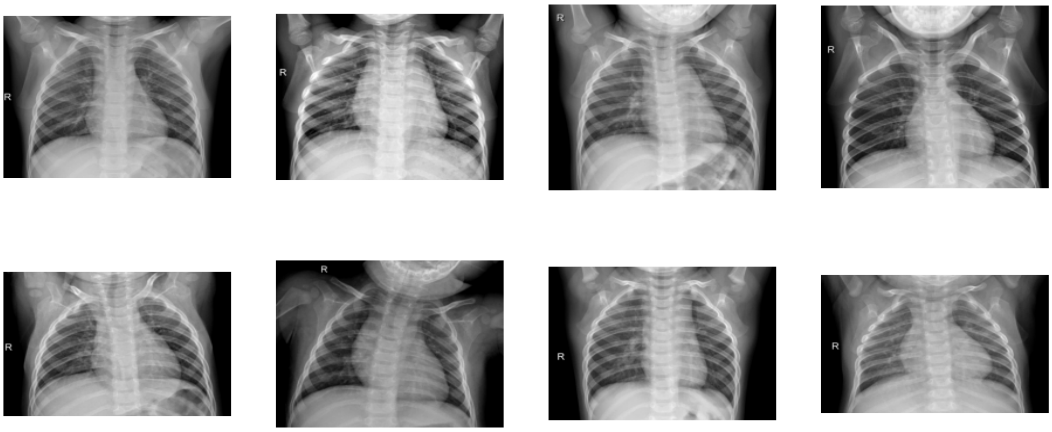

Fig. (1). Normal Images.

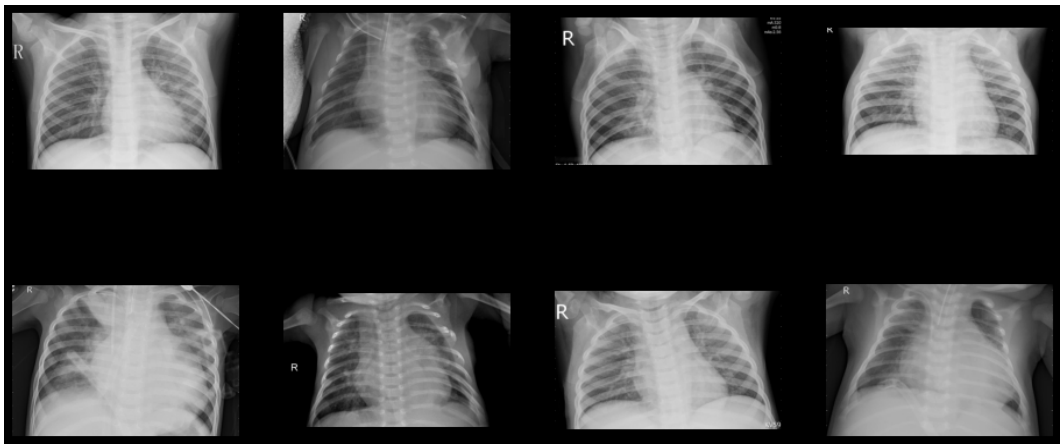

Fig. (2). Pneumonia Images.

Table 2. Details of Dataset.

Dataset Details					
Train		**Test**		**Validation**	
Normal	**Pneumonia**	**Normal**	**Pneumonia**	**Normal**	**Pneumonia**
1241	3775	234	390	112	112

3.2. Methodology

3.2.1. Importing the Dataset

The dataset can be downloaded from Kaggle easily. Its size is 3.9 GBs. We then need to check for the three directories to see if they have been downloaded successfully, and then respective directory names need to be set up for further use (Table **2**). The data division is responsible for ensuring that the model is built, fine-tuned, and evaluated in a controlled manner to mitigate the issue of overfitting. Overfitting refers to a situation where a model exhibits high performance on the training data but fails to generalize well to new, unseen data. The inclusion of a validation set serves to mitigate the risk of "data leakage" during the model's creation phase, as it provides an unbiased assessment. Conversely, the test set serves as the definitive gauge of the model's genuine ability to generalize.

The data division plays a crucial role in research by ensuring the integrity and dependability of machine learning models. It allows researchers to draw educated conclusions about the performance and capabilities of their models.

3.2.2. Preprocessing and Augmentation

Data augmentation techniques are employed to enlarge and enhance a dataset artificially. Overfitting problems can be fixed, and the model's generalization ability can be improved with this technique. First, to ensure that differences in image size would not influence the performance of the model, every image was resized to have a constant dimension of 224×224 pixels. Regardless of the image's actual size, this homogeneity enables the model to concentrate on its distinctive qualities. An image's pixel values are normalized using the rescale setting of 1/255. An image's original pixel values can be between 0 and 255. The pixel values

were converted to a scale from 0 to 1 by rescaling by a factor of 1/255. This phase ensures faster convergence during model training. Data augmentation techniques were employed to expand the dataset and improve model robustness artificially. The images are subjected to random shear transformations with a shear range of 0.2 and random zooming with a zoom range of 0.2. By using these techniques, the photos can be altered, broadening the training set's diversity. The default for the horizontal flip is 'True', which means that images are randomly flipped along their horizontal axis. The model may be trained to recognize pneumonia signs using this method, regardless of how they are oriented in the image. As part of the augmentation process, the resize procedure is used to either shrink or enlarge the image. Clipping the image angles anticlockwise by 0.2% shear range. The X-rays were randomly zoomed to a magnification ratio of 0.2 percent, and then they were flipped horizontally.

3.2.3. Model

Feature extractors and the classifier form the backbone of the model. In a feature extraction stack, the output of one layer feeds into the input of the next layer. In this, the authors suggest a three-layer architecture with convolution, max-pooling, and classification layers. The various levels are as follows: Figs. (**3** and **4**) represents the details of the model design flowchart and CNN model, which is used for feature extraction (Tables **3** and **4**). The base layer requires 224x224 pixel images with 3 colour channels. In order to capture complex patterns, the successive layers perform a sequence of convolutional procedures followed by max-pooling, thereby progressively decreasing the spatial dimensions while increasing the number of channels. The model makes use of independent convolutions to facilitate rapid feature acquisition. To maintain consistency throughout training, batch normalization is applied after specific convolutions. The architecture is made up of many convolutional blocks of progressively greater depth piled on top of one another, with the reduction of spatial dimensions being completed by max-pooling layers. Next, the input is transformed into a vector by a flattening layer, and then dense (completely connected) layers are added. Overfitting can be reduced with the use of dropout layers. Since the final dense layer produces only two classes, it's best used for simple classification problems. In order to learn complicated visual data and produce precise predictions, this CNN model employs a hierarchical pattern extraction.

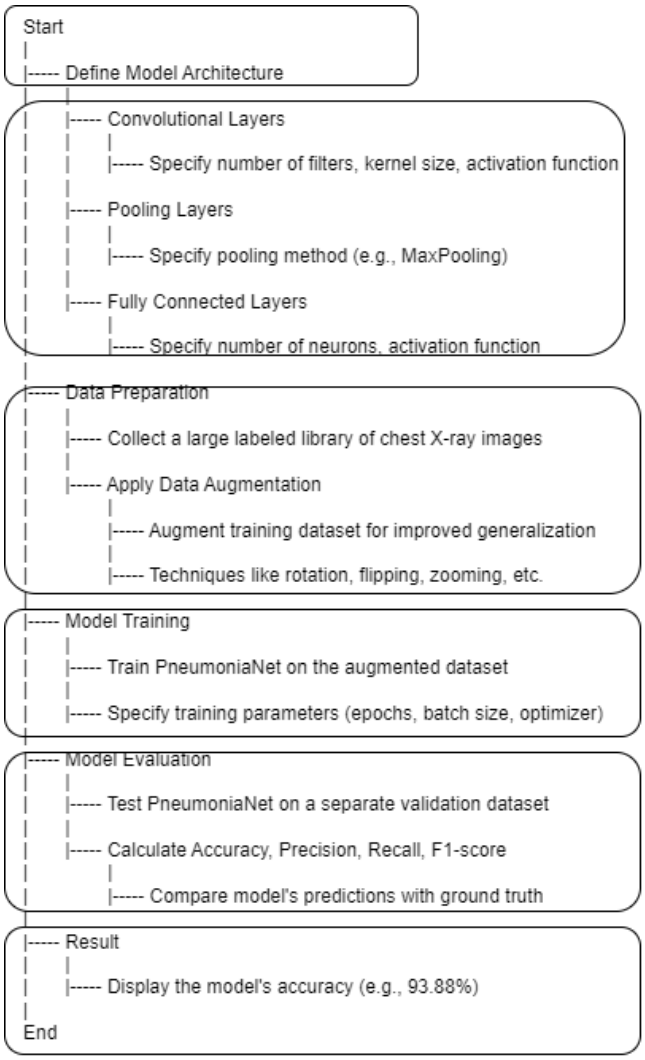

Fig. (3). Model Design flowchart. (*A higher resolution/colour version of this figure is available in the electronic copy of the article*).

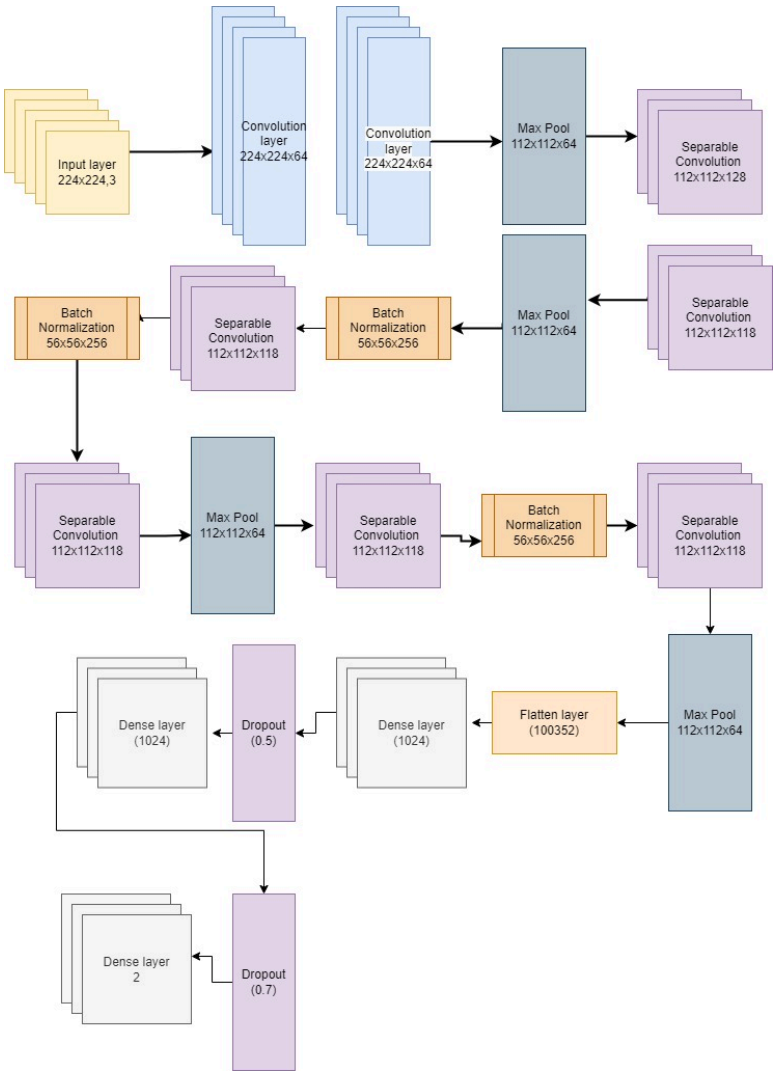

Fig. (4). CNN model architecture. (*A higher resolution/colour version of this figure is available in the electronic copy of the article*).

Table 3. The CNN Model.

Layer	Number	Shape
Input Layer	-	224×224, 3
Convolution	2	(224×224×64)
Max Pool	1	(112×112×64)
Separable Convolution	2	(112×112×128)
Max Pool	1	(56×56×128)
Separable Convolution	1	(56×56×256)
Batch Normalization	1	(56×56×256)
Separable Convolution	1	(56×56×256)
Batch Normalization	1	(56×56×256)
Separable Convolution	1	(56×56×256)
Max Pool	1	(28×28×256)
Separable Convolution	1	(28×28×512)

(Table 1) contd….

Layer	Number	Shape
Batch Normalization	1	(28×28×512)
Separable Convolution	1	(28×28×512)
Batch Normalization	1	(28×28×512)
Separable Convolution	1	(28×28×512)
Max Pool	1	(14×14×512)
Flatten Layer	1	(100352)
Dense Layer	1	(1024)
Dropout (0.5)	1	(1024)
Dense	1	(512)
Dropout (0.7)	1	(512)
Dense	1	(2)

Table 4. Parameters of the Model.

Parameter Type	Number
Non-trainable Parameters	3,072
Trainable Parameters	104,194,434
Total Parameters	104,197,506

3.2.4. Training

The model was trained on Google Colab with Nvidia Tesla K80. Each iteration took approximately 550s. To strike a good balance between training time, convergence, and model performance, 100 epochs were run. Multiple factors, including convergence, reducing overfitting and underfitting, computational resources, and validation results, informed the decision to employ 100 epochs. The model can undergo enough training iterations to capture important characteristics in the data while minimizing overfitting when 100 epochs are used in the training process. The parameters used for training are tabulated in Table **5.**

Table 5. Parameters of training.

Parameter	Value
Batch Size	14
Epochs	50
Early Stopping	NA
Learning Rate Reduction	0.8 after 5 epochs
Loss	Binary Cross Entropy
Metrics	Accuracy
Learning Rate	0.0001
Optimizer	Adam
Steps Per Epoch	500
Validation Steps Per Epoch	10

4. EXPERIMENT AND RESULT ANALYSIS

To train the PneumoniaNet model, a number of epochs were executed to fine-tune the network's parameters iteratively. The training set is analyzed in a single epoch, and then the model is put to the test on the validation set. In this experiment, 100 epochs were used, and after each epoch, the model's accuracy and loss values were recorded for both the training and validation sets. A validation set was utilized to ensure the model was robust in the face of new data and to prevent overfitting. The model's ability to generalize to new data is tested using the validation set, a subset of the training data that is not used for training. True outcomes (both positive and negative) as a percentage of the total population is what we call accuracy. It's a metric for assessing the precision with which the instances are sorted. The loss value, on the other hand, quantifies the extent to which the model over- or under-predicted. A lower loss value indicates a better model fit. Figs. (**5** and **6**) show the accuracy and loss, respectively.

Fig. (5). Accuracy. (*A higher resolution/colour version of this figure is available in the electronic copy of the article*).

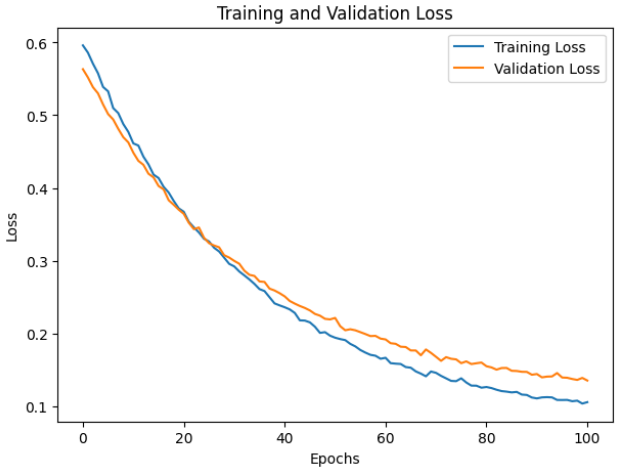

Fig. (6). Loss. (*A higher resolution/colour version of this figure is available in the electronic copy of the article*).

Over the training epochs, the model's accuracy in correctly classifying images improved, as measured by the training accuracy measure. As the model learned and then consolidated its knowledge, its accuracy gradually improved until leveling out. Similar to the training accuracy, the validation accuracy rose steadily over time. It appeared that the model was not overfitting and generalized well to new data because the validation accuracy was so close to the training accuracy. Maximum training accuracy was 93.47%, with maximum validation accuracy of 90.45%. As the model gets better, it should be no surprise that both the training loss and the validation loss decreased over time. As with precision, the rate at which loss decreased was steepest in the early epochs before leveling out. This indicated that the model was improving its fit to the data as the prediction error decreased. PneumoniaNet showed promising performance in appropriately classifying the chest X-ray images while avoiding overfitting. The positive trends in accuracy and loss values over epochs suggest that the model is learning and generalizing competently.

PneumoniaNet was evaluated using four criteria (Accuracy, Precision, Recall, and F1-Score) and compared to six other state-of-the-art models. CheXNet, DenseNet, InceptionNet, ResNet, VGGNet, and COVID-Net were some of the models used. The models were evaluated to see how well they perform for detecting and classifying pneumonia, given each has been utilized in medical imaging for a variety of illness detection tasks, including PneumoniaNet. Table **6** presents a comparative performance of all the seven models:

When compared to the other models, PneumoniaNet had the best results across all metrics tested. This finding confirms that the PneumoniaNet model is a reliable and useful tool for identifying pneumonia in chest X-ray images.

For each of these models, the confusion matrix was also computed. It's a four-cell table that reports the number of FP (False Positives), FN (False Negatives), TP (True Positives), and TN (True Negatives). This opens the door to in-depth research beyond the simple measurement of accuracy in classification. Since accuracy might be deceptive when the data set is uneven (*i.e.*, when the number of observations in each class varies substantially), it is not a good indicator of a classifier's true performance. PneumoniaNet's improved performance was further validated by an evaluation utilizing confusion matrices.

PneumoniaNet outperforms other state-of-the-art models in the identification and classification of pneumonia from chest X-ray images due to its sophisticated convolutional neural network architecture and training technique. PneumoniaNet can be further refined and validated with additional illness types and data sets in the future. Here's a detailed explanation of the confusion matrix values for each model:

5. DISCUSSION

PneumoniaNet achieved a high number of True Positives, correctly identifying 223 cases of pneumonia. However, it had a relatively low count of False Positives (11), indicating a good ability to avoid misclassifying healthy cases as pneumonia. It did, however, miss out on identifying 30 cases of pneumonia (False Negatives). On the positive side, it accurately classified 360 healthy cases as healthy (True Negatives). This model's high Precision (97.03%) suggests it is effective at avoiding false positives, and its high Recall (92.30%) indicates its ability to capture a significant portion of actual pneumonia cases, as shown in Fig. (**7**).

CheXNet demonstrated 200 True Positives, which means it correctly identified pneumonia in these cases. However, it had a higher count of False Positives (34), indicating a tendency to sometimes classify healthy cases as pneumonia. It missed 50 instances of pneumonia (False Negatives). The model did accurately classify 340 healthy cases as healthy (True Negatives). CheXNet's Precision (90.90%) indicates a relatively lower ability to avoid false positives, and its Recall (87.20%) suggests that it captured a lower proportion of actual pneumonia cases compared to PneumoniaNet, as shown in Fig. (**8**).

Table 6. Comparative Performance of the model.

Model	Accuracy	Precision	Recall	F1-Score	Sensitivity	Specificity
PneumoniaNet	93.88%	97.03%	92.30%	0.94	88.14%	97.04%
CheXNet	86.60%	90.90%	87.20%	0.89	80.00%	90.91%
DenseNet	88.20%	92.20%	88.50%	0.90	82.00%	92.25%
InceptionNet	91.30%	94.90%	91.00%	0.92	86.00%	94.92%
ResNet	89.70%	93.60%	89.70%	0.91	84.00%	93.58%
VGGNet	86.60%	90.90%	87.20%	0.89	80.00%	90.91%
COVID-Net	89.70%	93.60%	89.70%	0.91	84.00%	93.58%

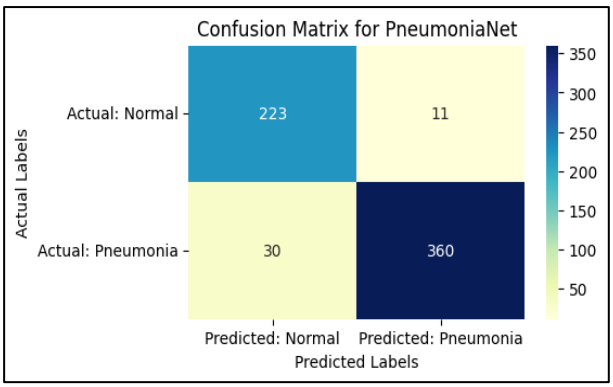

Fig. (7). CM for PneumoniaNet. (*A higher resolution/colour version of this figure is available in the electronic copy of the article*).

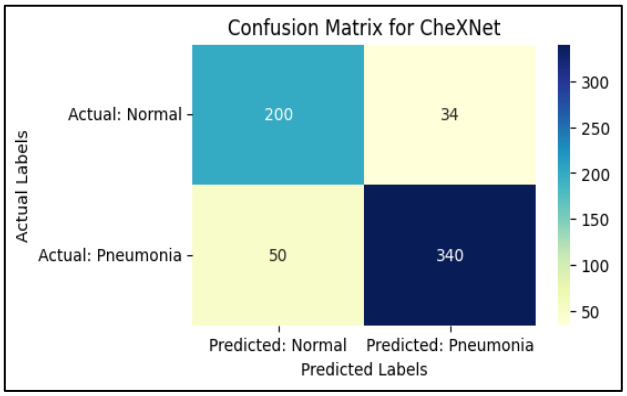

Fig. (8). CM for CheXNet. (*A higher resolution/colour version of this figure is available in the electronic copy of the article*).

DenseNet achieved 205 True Positives, indicating accurate identification of pneumonia cases. It had 29 False Positives, suggesting some misclassification of healthy cases as pneumonia. The model missed 45 cases of pneumonia (False Negatives) and correctly classified 345 healthy cases (True Negatives). The Precision (92.20%) and Recall (88.50%) values indicate a good balance between avoiding false positives and capturing true positives, as shown in Fig. (**9**).

InceptionNet's True Positives numbered 215, showing effective pneumonia identification. It had 19 False Positives, indicating a relatively lower rate of misclassifying healthy cases. The model missed 35 instances of pneumonia (False Negatives) and accurately classified 355 healthy cases (True Negatives). InceptionNet's high Precision (94.90%) and Recall (91.00%) values suggest a strong balance between avoiding false positives and capturing true positives, as shown in Fig. (**10**).

ResNet correctly identified 210 pneumonia cases (True Positives) while having 24 False Positives, indicating a moderate rate of misclassifying healthy cases. It missed 40 instances of pneumonia (False Negatives) and accurately classified 350 healthy cases (True Negatives). ResNet's Precision (93.60%) and Recall (89.70%) values suggest a trade-off between avoiding false positives and capturing true positives, as shown in Fig. (**11**).

VGGNet achieved 200 True Positives, indicating accurate pneumonia identification. It had 34 False Positives, suggesting misclassification of some healthy cases. The model missed 50 instances of pneumonia (False Negatives) and accurately classified 340 healthy cases (True Negatives). VGGNet's Precision (90.90%) and Recall (87.20%) values indicate performance similar to CheXNet, as shown in Fig. (**12**).

COVID-Net correctly identified 210 pneumonia cases (True Positives) while having 24 False Positives, indicating a moderate rate of misclassification of healthy cases. It missed 40 instances of pneumonia (False Negatives) and accurately classified 350 healthy cases (True Negatives). COVID-Net's Precision (93.60%) and Recall (89.70%) values are similar to ResNet's performance as shown in Fig. (**13**).

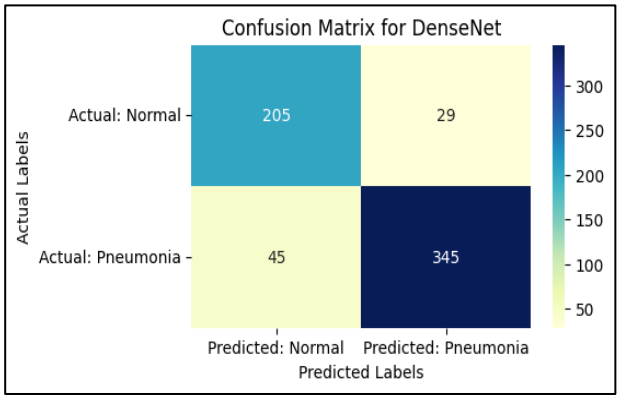

Fig. (9). CM for DenseNet. (*A higher resolution/colour version of this figure is available in the electronic copy of the article*).

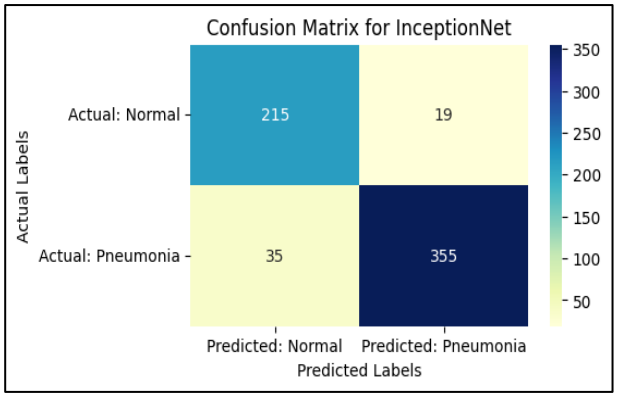

Fig. (10). CM for InceptionNet. (*A higher resolution/colour version of this figure is available in the electronic copy of the article*).

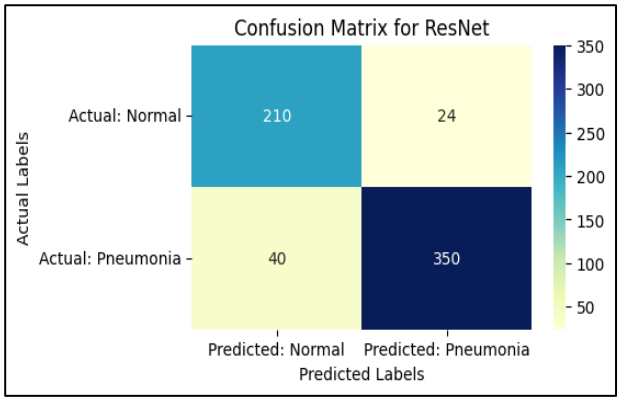

Fig. (11). CM for ResNet. (*A higher resolution/colour version of this figure is available in the electronic copy of the article*).

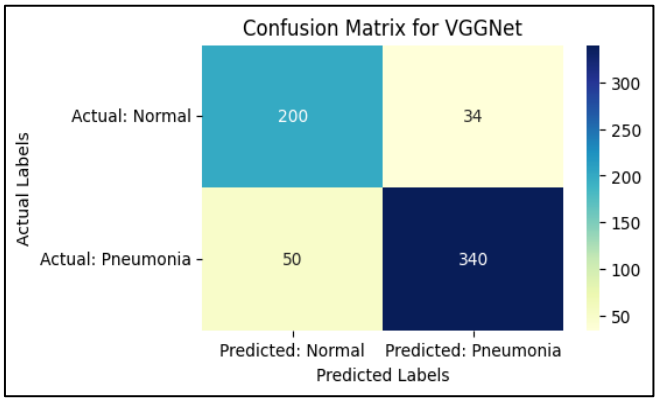

Fig. (12). CM for VGGNet. (*A higher resolution/colour version of this figure is available in the electronic copy of the article*).

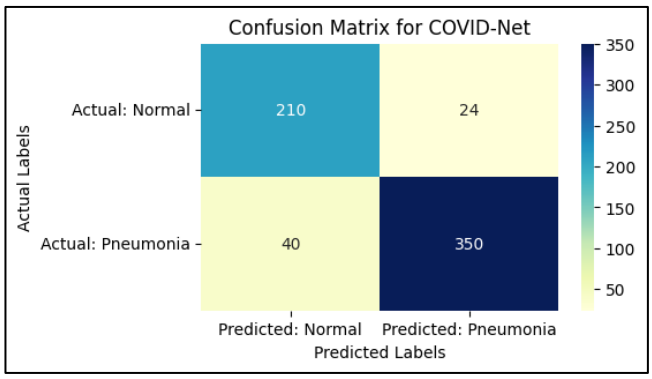

Fig. (13). CM for COVID-Net. (*A higher resolution/colour version of this figure is available in the electronic copy of the article*).

CONCLUSION

In this research, we introduced PneumoniaNet, a novel Convolutional Neural Network (CNN) model trained on chest X-ray images to detect and categorize pneumonia. Several state-of-the-art models were used to assess PneumoniaNet's efficacy; these were CheXNet, DenseNet, InceptionNet, ResNet, VGGNet, and COVID-Net. Accuracy, precision, recall, and F1-score were the metrics where PneumoniaNet excelled in comparison to other models. CheXNet, DenseNet, InceptionNet, ResNet, VGGNet, and COVID-Net were among the models compared to the suggested technique. Accuracy, precision, recall, F1-score, sensitivity, and specificity are some of the measures used. When compared to other models, PneumoniaNet has the highest accuracy at 93.88%.With a precision of 97.03%, PneumoniaN*et al*so shows that it can make the fewest erroneous predictions. PneumoniaNet's recall (sensitivity) of 92.30% demonstrates its efficacy in spotting a sizable fraction of genuine positives.

PneumoniaNet's F1-score of 94.61% exemplifies a fair compromise between accuracy and recall. PneumoniaNet has a sensitivity of 88.14 percent, which means it can reliably identify positive cases.PneumoniaNet has a high level of accuracy in identifying false negatives, with a specificity of 97.04%. When compared to these criteria, other models do poorly. The accuracy, precision, recall, F1-score, sensitivity, and specificity of various networks, such as CheXNet, DenseNet, InceptionNet, ResNet, VGGNet, and COVID-Net, are all different. When taken as a whole, these indicators prove that PneumoniaNet is the best system available for identifying and classifying pneumonia patients. This result demonstrates that PneumoniaNet was successfully trained to recognize and accurately classify chest X-ray pictures for evidence of pneumonia.

Moving forward, several key areas of future work can enhance the impact of PneumoniaNet. Expanding the dataset's size and diversity, exploring transfer learning for quicker convergence, integrating multi-modal data, and enhancing model explainability are essential steps. Further efforts to improve the model's robustness, address bias concerns, and collaborate with medical experts will ensure its clinical relevance. Real-time deployment optimization, subtype differentiation, and extension to other thoracic diseases offer exciting possibilities, promising a comprehensive AI solution that significantly advances early diagnosis and patient care in radiology.

While the study's findings are encouraging, it's important to note a few caveats. First, PneumoniaNet was mostly tested on one dataset, therefore, its results may not apply to other types of patients or imaging modalities. Second, it's possible that critical information is being left out if only chest X-rays are used. Lacking a way to convey its predictions to doctors, the model's interpretability also remains a barrier. Potential data biases were not thoroughly investigated, which limits the study's relevance to the real world. Finally, while PneumoniaNet's accuracy is impressive, it is still possible for false positives and negatives to occur; care should be taken, and more validation should be conducted before clinical integration.

Given the larger context of pneumonia infections, it is important to recognize that our current research focuses on classifications, which limits its scope. Pneumonia has many types, each with its own symptoms and diagnostic challenges. We categorize pneumonia using the two classifications in our study. We acknowledge the presence of different pneumonia types that warrant further study. Viral, aspiration, and atypical pneumonia, among others, present different diagnostic and classification issues. Our study provides a foundation for classifying different pneumonias using similar methods. Our study may help future researchers develop pneumonia disease-specific models and diagnostic approaches. Deep learning, convolutional neural networks, and robust evaluation criteria can improve pneumonia diagnosis across more types. Future studies should broaden these approaches to include more categories to create a comprehensive and effective diagnostic framework for pneumonia infections from multiple sources.

LIST OF ABBREVIATIONS

CNN = Convolutional Neural Network

DNN = Deep Neural Network

ETHICS APPROVAL AND CONSENT TO PARTICIPATE

Not applicable.

HUMAN AND ANIMAL RIGHTS

Not applicable.

CONSENT FOR PUBLICATION

Not applicable.

AVAILABILITY OF DATA AND MATERIALS

The authors confirm that the data supporting the findings of this research are available within the article.

FUNDING

None.

CONFLICT OF INTEREST

The authors declare no conflict of interest, financial or otherwise.

ACKNOWLEDGEMENTS

Declared none.

REFERENCES

[1] O. Ruuskanen, E. Lahti, L.C. Jennings, and D.R. Murdoch, "Viral pneumonia", *Lancet,* vol. 377, no. 9773, pp. 1264-1275, 2011. http://dx.doi.org/10.1016/S0140-6736(10)61459-6 PMID: 21435708

[2] L.A. Mandell, R.G. Wunderink, A. Anzueto, J.G. Bartlett, G.D. Campbell, N.C. Dean, S.F. Dowell, T.M. File Jr, D.M. Musher, M.S. Niederman, A. Torres, and C.G. Whitney, "Infectious Diseases Society of America/American Thoracic Society consensus guidelines on the management of community-acquired pneumonia in adults", *Clin. Infect. Dis.,* vol. 44, no. Suppl 2, suppl. Suppl. 2, pp. S27-S72, 2007. http://dx.doi.org/10.1086/511159 PMID: 17278083

[3] R.G. Wunderink, and G. Waterer, "Advances in the causes and management of community acquired pneumonia in adults", *BMJ,* vol. 358, p. j2471, 2017. http://dx.doi.org/10.1136/bmj.j2471 PMID: 28694251

[4] H.Y.F. Wong, H.Y.S. Lam, A.H.T. Fong, S.T. Leung, T.W.Y. Chin, C.S.Y. Lo, M.M.S. Lui, J.C.Y. Lee, K.W.H. Chiu, T.W.H. Chung, E.Y.P. Lee, E.Y.F. Wan, I.F.N. Hung, T.P.W. Lam, M.D. Kuo, and M.Y. Ng, "Frequency and distribution of chest radiographic findings in patients positive for COVID-19", *Radiology,* vol. 296, no. 2, pp. E72-E78, 2020. http://dx.doi.org/10.1148/radiol.2020201160 PMID: 32216717

[5] Y. LeCun, Y. Bengio, and G. Hinton, "Deep learning", *Nature,* vol. 521, no. 7553, pp. 436-444, 2015. http://dx.doi.org/10.1038/nature14539 PMID: 26017442

[6] G. Litjens, T. Kooi, B.E. Bejnordi, A.A.A. Setio, F. Ciompi, M. Ghafoorian, J.A.W.M. van der Laak, B. van Ginneken, and C.I. Sánchez, "A survey on deep learning in medical image analysis", *Med. Image Anal.,* vol. 42, pp. 60-88, 2017. http://dx.doi.org/10.1016/j.media.2017.07.005 PMID: 28778026

[7] T. Ozturk, M. Talo, E.A. Yildirim, U.B. Baloglu, O. Yildirim, and U. Rajendra Acharya, "Automated detection of COVID-19 cases using deep neural networks with X-ray images", *Comput. Biol. Med.,* vol. 121, p. 103792, 2020. http://dx.doi.org/10.1016/j.compbiomed.2020.103792 PMID: 32568675

[8] L. Wang, Z.Q. Lin, and A. Wong, "COVID-Net: a tailored deep convolutional neural network design for detection of COVID-19 cases from chest X-ray images", *Sci. Rep.,* vol. 10, no. 1, p. 19549, 2020. http://dx.doi.org/10.1038/s41598-020-76550-z PMID: 33177550

[9] I.D. Apostolopoulos, and T.A. Mpesiana, "COVID-19: automatic detection from X-ray images utilizing transfer learning with convolutional neural networks", *Phys. Eng. Sci. Med.,* vol. 43, no. 2, pp. 635-640, 2020. http://dx.doi.org/10.1007/s13246-020-00865-4 PMID: 32524445

[10] S. Singh, S.S. Rawat, M. Gupta, B.K. Tripathi, F. Alanzi, A. Majumdar, P. Khuwuthyakorn, and O. Thinnukool, *Deep attention network for pneumonia detection using Chest X-Ray images.,* vol. 74, no. 1, pp. 1673-1691, 2023. http://dx.doi.org/10.32604/cmc.2023.032364

[11] M. Bhandari, T.B. Shahi, B. Siku, and A. Neupane, "Explanatory classification of CXR images into COVID-19, Pneumonia and Tuberculosis using deep learning and XAI", *Comput. Biol. Med.,* vol. 150, p. 106156, 2022. http://dx.doi.org/10.1016/j.compbiomed.2022.106156

[12] F. Hajjej, S. Ayouni, M. Hasan, and T. Abir, "Automatic detection of cases of COVID-19 pneumonia from chest X-ray images and deep learning approaches", *Comput Intell Neurosci.,* vol. 2022, p. 7451551, 2022. http://dx.doi.org/10.1155/2022/7451551

[13] C.A. Ortiz-Toro, A. Garcia-Pedrero, M. Lillo-Saavedra, and C. Gonzalo-Martin, "Textural features for automatic detection and categorisation of pneumonia in chest X-ray images", *In. IEEE 35th Int. Sympo. Comp. Based Med. Syst.,* Shenzen, China, 2022, pp. 19-24. http://dx.doi.org/10.1109/CBMS55023.2022.00011

[14] K. Aktas, V. Ignjatovic, D. Ilic, M. Marjanovic, and G. Anbarjafari, "Deep convolutional neural networks for detection of abnormalities in chest X-rays trained on the very large dataset", *Signal Image Video Process.,* 2023, 17(4), 1035-1041. http://dx.doi.org/10.1007/s11760-022-02309-w PMID: 35873389

[15] P. Saxena, S.K. Singh, G. Tiwary, Y. Mittal, and I. Jain, "An artificial intelligence technique for Covid-19 detection with eXplainability using Lungs X-Ray Images", *In. IEEE International Conference on Distributed Computing and Electrical Circuits and Electronics (ICDCECE),* Ballari, India, 2022, pp. 1-6. http://dx.doi.org/10.1109/ICDCECE53908.2022.9793240

[16] D. Lv, Y. Wang, S. Wang, Q. Zhang, W. Qi, Y. Li, and L. Sun, "A Cascade-SEME network for COVID□19 detection in chest x-ray images", *Med. Phys.,* vol. 48, no. 5, pp. 2337-2353, 2021. http://dx.doi.org/10.1002/mp.14711 PMID: 33778966

[17] H.I. Hussein, A.O. Mohammed, M.M. Hassan, and R.J. Mstafa, "Lightweight deep CNN-based models for early detection of COVID-19 patients from chest X-ray images", *Expert Syst. Appl.,* vol. 223, p. 119900, 2023. http://dx.doi.org/10.1016/j.eswa.2023.119900 PMID: 36969370

[18] A. Iqbal, M. Usman, and Z. Ahmed, "Tuberculosis chest X-ray detection using CNN-based hybrid segmentation and classification approach", *Biomed. Signal Process. Control,* vol. 84, p. 104667, 2023. http://dx.doi.org/10.1016/j.bspc.2023.104667

[19] W. Kusakunniran, P. Borwarnginn, T. Siriapisith, S. Karnjanapreechakorn, K. Sutassananon, T. Tongdee, and P. Saiviroonporn, "Detecting COVID-19 in chest X-ray images", *IJECE,* vol. 13, no. 3, pp. 3290-3298, 2023. http://dx.doi.org/10.11591/ijece.v13i3.pp3290-3298

[20] D.E. Cahyani, A.D. Hariadi, F.F. Setyawan, L. Gumilar, and S. Setumin, "COVID-19 classification using CNN-BiLSTM based on chest X-ray images", *Bull. Electr. Eng. Inform.,* vol. 12, no. 3, pp. 1773-1782, 2023. http://dx.doi.org/10.11591/eei.v12i3.4848

[21] D. Mitra, P. Rakshit, A. Jha, D. Dugar, and K. Iqbal, "Lung disease prediction using deep learning", *Adv. Commun., Devices Network.: Proceed. ICCDN 2021.,* 2023. http://dx.doi.org/10.1007/978-981-19-2004-2_40

[22] M. Nahiduzzaman, M.R. Islam, and R. Hassan, "ChestX-Ray6: Prediction of multiple diseases including COVID-19 from chest X-ray images using convolutional neural network", *Expert Syst. Appl.,* vol. 211, p. 118576, 2023. http://dx.doi.org/10.1016/j.eswa.2022.118576 PMID: 36062267

[23] S.H. Karaddi, and L.D. Sharma, "Automated multi-class classification of lung diseases from CXR-images using pre-trained convolutional neural networks", *Expert Syst. Appl.,* vol. 211, p. 118650, 2023. http://dx.doi.org/10.1016/j.eswa.2022.118650

[24] T. Agrawal, and P. Choudhary, "ALCNN: Attention based lightweight convolutional neural network for pneumothorax detection in

chest X-rays", *Biomed. Signal Process. Control,* vol. 79, p. 104126, 2023.
http://dx.doi.org/10.1016/j.bspc.2022.104126

[25] Li. Yao, E. Poblenz, D. Dagunts, B. Covington, D. Bernard, and K. Lyman, "Learning to diagnose from scratch by exploiting dependencies among labels", *arXiv,* 2017.

[26] H. Boussaid, and I. Kokkinos, "Fast and exact: ADMM-based discriminative shape segmentation with loopy part models", *Proceedings of Conference on Computer Vision and Pattern Recognition (CVPR),* 2014 Columbus, OH, USA
http://dx.doi.org/10.1109/CVPR.2014.517